Effect of interaction between potassium and structural promoters on Fischer–Tropsch performance in iron-based catalysts

Guoyan Zhao [a,b], Chenghua Zhang [a,*], Shaodong Qin [a,b], Hongwei Xiang [a], Yongwang Li [a]

[a] State Key Laboratory of Coal Conversion, Institute of Coal Chemistry, Chinese Academy of Sciences, Taiyuan 030001, People's Republic of China
[b] Graduate University of Chinese Academy of Sciences, Beijing 100039, People's Republic of China

ARTICLE INFO

ABSTRACT

The Fischer–Tropsch synthesis (FTS) performances of iron-based catalysts promoted with/without potassium compounds containing different acidic structural promoters (Al_2O_3, SiO_2, and ZSM-5) were studied in this research. Characterization technologies of temperature-programmed reduction with CO (CO-TPR), powder X-ray diffraction (XRD) and Mössbauer effect spectroscopy (MES) were used to study the effect of K–structural promoter interactions on the carburization behaviors of catalysts. It showed that the addition states of potassium (K–Al_2O_3, K–SiO_2, K–ZSM-5 and K-free) have a significant influence on the formation of iron carbides, which shows a following sequence in promotion of carburization: K–Al_2O_3 > K–SiO_2 > K–ZSM-5 > K-free. The FTS reaction test was performed in a fixed bed reactor. It is found that Fe/K–Al_2O_3 catalyst leads to the highest CO conversion, Fe/K–ZSM-5 catalyst shows the highest H_2 conversion, and Fe/K-free catalyst shows the lowest CO and H_2 conversion. As for the hydrocarbon selectivity, Fe/K–SiO_2 catalyst yields the lowest methane and the highest C_5^+ products, Fe/K–ZSM-5 catalyst yields higher methane and the highest liquid hydrocarbon product, whereas Fe/K-free catalyst yields the highest methane and the lowest C_5^+ products. These results can be explained from the interaction between potassium and structure promoters, and the spillover of reactants or intermediates from Fe sites to the surfaces of structural promoters.

© 2008 Elsevier B.V. All rights reserved.

1. Introduction

Fischer–Tropsch synthesis (FTS) has been recognized as an important technology in the production of liquid fuels and chemicals from syngas derived from coal, natural gas, and other carbon-containing materials [1]. With the emergency of transportation fuel shortage in the whole world and the pollution from the combustion of fuels refined from petroleum, FTS is becoming a much concerned academic or industrial topic for more and more people, especially in China [2]. The current focus on the FTS process deals with the production of transportation fuels such as gasoline and diesel [3], which can be maximized via oligomerization or hydrocracking of FTS effective hydrocarbons (ethene, propylene or wax). However, traditional FTS iron-based catalysts produce a large amount of methane and gaseous alkanes, which are useless for the utilization of coal or natural gas resources. Therefore, it is expected that more effective hydrocarbons are produced via selectivity control, addition of promoters or some other feasible ways.

It is well known that the promotion of potassium has significant effect on the FTS performance of catalysts [4–7]. That is,

potassium suppresses the production of methane and improves the effective hydrocarbon selectivity. Dry and Oosthuizen [8] studied the correlation between catalysts surface basicity and hydrocarbon selectivity, and found that the surface basicity can apparently suppress the methane selectivity. Alkali potassium can bring high surface basicity to the catalysts, but the acidic sites of structural promoter suppress surface basicity. Bukur et al. [9] studied the effect of potassium on the silica-supported iron catalysts and found that silica can suppress the basicity of the K promoter. Dlamini et al. [10] studied the effect of adding SiO_2 to a precipitated-iron catalyst using scanning electron microscopy analyses and found that the amount of effective K_2O associated with Fe is less when SiO_2 added as a binder. In Yong et al.'s study [11], a potassium-containing catalyst without SiO_2 addition possesses a markedly higher activity than the catalysts containing SiO_2. The decreased activity with addition of SiO_2 was attributed by authors to the decrease of the effective potassium due to the interaction between potassium and silica. More recently, Zhang et al. [1] observed a much more complex interaction between metal components (Fe, Cu, K) and SiO_2, which had an apparent effect on the surface properties and FTS performance of catalysts. Similarly, this kind of interaction between potassium and structural promoters was observed in other supported catalysts. For example, an interaction between potassium and alumina exists in alumina-supported cata-

lysts. Many researchers postulated that the interaction is in a phase of $KAlO_2$, and Kotarba [12] studied the role of $KAlO_2$ phase and the chemical state of potassium in iron catalysts using model compounds ($KAlO_2$ and $KFeO_2$) and found that potassium at the surface of catalyst is ionic on $KAlO_2$ and covalent on $KFeO_2$. Jun et al. [13] investigated three iron catalysts with different supports (without support, alumina-supported and silica-supported) for FTS reaction. Their results indicated that Al_2O_3 can dilute and SiO_2 can severely dilute the potassium promotion using temperature-programmed decarburization, whereas Al_2O_3 can help the dispersion of K on Fe-alumina catalyst and SiO_2 makes the K and Fe dispersion worse. Ma et al. [14] studied potassium effects on activated-carbon-supported iron catalysts and this report also indicates that the AC-supported iron catalysts need more of potassium promoter to increase catalyst activity relative to the precipitated-iron catalyst due to the dispersion effect of AC support.

A lot of literature had proved that an interaction between potassium and structural promoters exists in iron-based FTS catalysts. However, little work was conducted to purposefully study the effect of this interaction on the FTS performance. The present work focuses on the interaction between potassium and some structural promoters, and its effect on FTS performances (carburization behavior, activity, stability, and selectivity) of an iron-based catalyst. The structural promoters (SiO_2, Al_2O_3, and ZSM-5) with different intrinsic acidities were used to counteract the surface basicity of potassium promoter and to provide different K–structural promoter interactions.

2. Experimental

2.1. Catalysts preparation

The FeMn–SiO_2 precursor used in present study was prepared by a combination method of continuous co-precipitation and spray-drying technology, detailed making method is described in literature [1]. Then potassium promoter with Fe/K mole ratio of 100/3 was added to the precursor using the method of mechanically mixed with the different compounds of potassium: K–ZSM-5, K–SiO_2 and K–Al_2O_3. These catalysts were signed as Fe/K-free, Fe/K–ZSM-5, Fe/K–SiO_2, and Fe/K–Al_2O_3 separately, and the detailed description of catalysts is presented in Table 1.

2.2. Reactor system and operation procedure

The experiments were conducted in a 12 mm i.d. stainless steel fixed bed reactor with an effective bed length of approximately 15 cm (15 cm^3 bed volume). For all the experiments, approximately 3 g catalysts (20–40 mesh) were filled in the reactor, the remaining volume of reactor was filled with quartz granules with the diameter of 10–20 and 20–40 mesh. All the catalysts were reduced with

Table 1
Description of catalysts

Catalyst no.	Description
Fe/K-free	FeMn–SiO_2 blank sample was dried at 120 °C overnight and calcined at 500 °C for 5 h.
Fe/K–ZSM-5	Promoted with K–ZSM-5. K–ZSM-5 was prepared via ion-exchanging of H–ZSM-5 with a KOH solution, dried at 120 °C overnight and calcined at 500 °C for 5 h.
Fe/K–SiO_2	Promoted with K–SiO_2. K–SiO_2 was prepared from drying of potassium water glass at 120 °C overnight and calcined it at 500 °C for 5 h.
Fe/K–Al_2O_3	Promoted with K–Al_2O_3. K–Al_2O_3 was prepared with mixing a KOH solution with aluminous sol, dried at 120 °C overnight and calcined at 500 °C for 5 h.

syngas (H_2/CO = 2.0) at 280 °C, 0.5 MPa, and 1000 h^{-1} for 16 h, then the reactor was cooled down to 160 °C. Then the pressure of the system was set to 1.50 MPa, and the temperature was gradually increased to 250 °C by 10 °C/h. The time on steam of all catalysts is about 120 h. The product in the hot and cold traps were collected over 24 h, weighted and sampled for analysis. During every mass balance period, the tail gas was analyzed twice.

2.3. Catalysts characterization

Temperature-programmed reduction (TPR) was used to measure the rate of carburization of different K-promoted catalysts. Catalysts (80 mg) were loaded into a quartz tube reactor and first heated to 500 °C and kept for 30 min, and then cooled to ambient temperature in Helium gas. The flow was then switched to 5%CO/95%He and the reaction temperature was increased to 1000 °C at rate of 10 °C/min. The consumption of reactant gas was monitored by mass spectroscopy.

Powder X-ray diffraction (XRD) measurements were carried out using a D-5000 Siemens diffractometer and Cu Kα radiation (λ = 1.5406 Å).

The Mössbauer effect spectroscopy (MES) was used to test the structure of the catalysts after reduction and reaction, which measured with a CANBERRA Series 40 MCA constant-acceleration Mössbauer spectrometer (CANBERRA, USA) at room temperature, using a 25 m Ci^{57}Co in Pd matrix.

3. Results

3.1. CO-TPR

Fig. 1 is CO-TPR profiles of all catalysts. It can be seen that Fe/K-free, Fe/K–ZSM-5 and Fe/K–Al_2O_3 catalysts all have three reduction/carburization peaks and Fe/K–SiO_2 catalyst has two peaks. The first peak is in the temperature range of 200–300 °C which is ascribed to the reduction of Fe_2O_3 to Fe_3O_4. The second peak located in 400–550 °C is corresponding to the carburization of iron oxides, and the peak after 600 °C is corresponding to the carburization of the difficultly reduced iron oxide phase. The addition of potassium has a marked effect on these carburization peaks. That is, all states of potassium promoters move the reduction/carburization peaks to lower temperature and strengthen the peak intensity in different extents. Specifically, the addition of K–ZSM-5 is less promotional on the carburization, which only
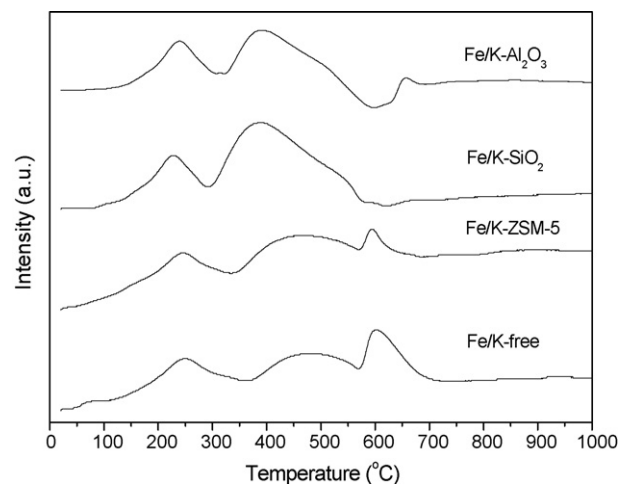

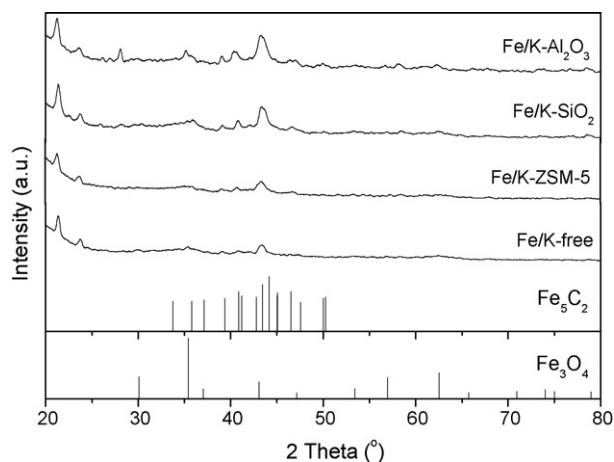**Fig. 1.** CO-TPR profiles of all four catalysts.

Fig. 2. XRD patterns of the catalysts after reaction.

Table 2
Mössbauer parameters of the catalysts after FTS reaction

Catalysts	Phase	Mössbauer parameters			
		IS (mm/s)	QS (mm/s)	Hhf (kOe)	Area (%)
Fe/K-free	χ-Fe$_5$C$_2$	0.40	−0.26	185	4.2
		0.22	0.22	218	11.0
		0.19	−0.16	105	6.2
	Fe^{3+}(spm)	0.30	0.94		69.3
	Fe^{2+}(spm)	1.02	1.66		9.2
Fe/K–ZSM-5	χ-Fe$_5$C$_2$	0.27	−0.16	186	11.7
		0.26	0.02	222	15.2
		0.13	0.03	108	6.8
	Fe^{3+}(spm)	0.38	0.87		51.3
	Fe^{2+}(spm)	0.94	1.64		15.1
Fe/K–SiO$_2$	χ-Fe$_5$C$_2$	0.26	−0.14	180	15.5
		0.25	0.01	219	19.1
		0.13	0.02	103	8.0
	Fe^{3+}(spm)	0.31	0.91		49.6
	Fe^{2+}(spm)	0.88	1.56		7.9
Fe/K–Al$_2$O$_3$	χ-Fe$_5$C$_2$	0.28	−0.13	183	23.1
		0.26	0.03	221	26.8
		0.11	0.04	106	14.4
	Fe^{3+}(spm)	0.28	0.87		21.7
	Fe^{2+}(spm)	0.95	1.46		14.0

Reaction condition: 250 °C, 1.50 MPa, H$_2$/CO = 2.0 and GHSV = 4000 h^{-1} for 120 h.

slightly lowers the reduction temperature of the peaks and weakens the intensity of the high-temperature peak. In contrast, the addition of K–SiO$_2$ and K–Al$_2$O$_3$ has much more apparent effects on the carburization. That is, the temperatures of the first and second peaks are lower 20 and 100 °C, respectively, for Fe/K–SiO$_2$ catalyst than for Fe/K-free catalyst. And, those for Fe/K–Al$_2$O$_3$ catalyst are lower 10 and 90 °C than for Fe/K-free catalyst. At the same time, K–SiO$_2$ eliminates the third peak at 600 °C. K–Al$_2$O$_3$ also eliminates the peak at 600 °C, whereas it causes another carburization peak at 650 °C. These results indicate that the addition of potassium promoters can restrain carburization of catalysts at high temperature, and make the catalyst carburize completely at lower temperature.

3.2. Catalyst samples after FTS reaction

The XRD patterns and MES spectra of the catalysts after reaction are shown in Figs. 2 and 3, and the MES parameters are presented in Table 2. Fig. 4 shows the content of phase composition of the catalysts after reaction. As shown in Fig. 2, the XRD patterns of all catalysts show two diffraction peaks below 25°, a broad diffraction peak at 36°, two weak peaks at 39° and 40° and a more prominent peak at 43°. According to JCPDS database, the two peaks below 25° correspond to the solid wax, which are not discussed here. The broad peak at 36° is ascribed to the iron oxide phase. The peaks at 39°, 40° and 43° correspond to the iron car-
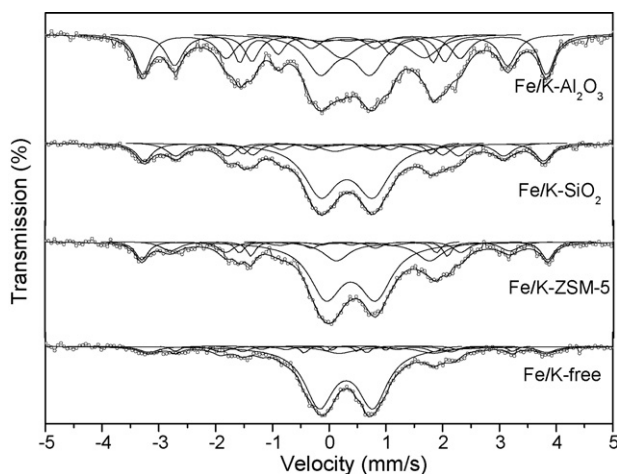
bide phase. The diffraction intensity of iron carbides increases in the orders: Fe/K-free < Fe/K–ZSM-5 < Fe/K–SiO$_2$ < Fe/K–Al$_2$O$_3$. The XRD patterns show the existence of iron carbides in catalysts after reaction, whereas it is difficult to distinguish the type of iron carbides due to the weak diffraction signal. However, the Mössbauer spectra can provide the type of iron phase and composition. From Fig. 3, the MES spectra of the potassium-promoted catalysts after reaction contain several sets of sextets and doublets. The sextets with Hhf of 184 ± 3 kOe, 222 ± 3 kOe and 110 ± 6 kOe can be attributed to the Hägg carbide, χ-Fe$_5$C$_2$ [15]. The spectral parameters of two doublets can be attributed to the trivalent and bivalent iron oxides in superparamagnetic state in small crystallites, respectively [4]. Table 2 shows the accurate content of every iron phase. For Fe/K-free, Fe/K–ZSM-5 and Fe/K–SiO$_2$, Fe^{3+} take the most part of the compositions, which content are more than 50%. But for Fe/K–Al$_2$O$_3$, Fe^{3+} is less than 25% and χ-Fe$_5$C$_2$ take the most part of the compositions, which has the content of 64.3%. Fig. 4 shows the variation of each phase composition. The content of carbide in four catalysts show the following sequence: Fe/K-free < Fe/K–ZSM-5 < Fe/K–SiO$_2$ < Fe/K–Al$_2$O$_3$, which is constant with the XRD results.

Fig. 3. Mössbauer spectra of the potassium-promoted iron-based catalysts after reaction.
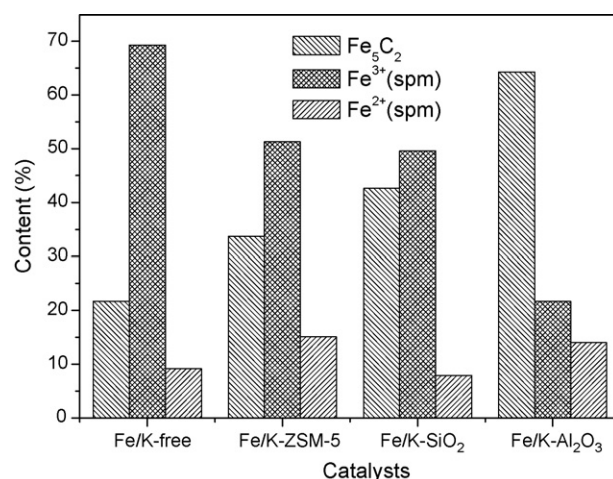

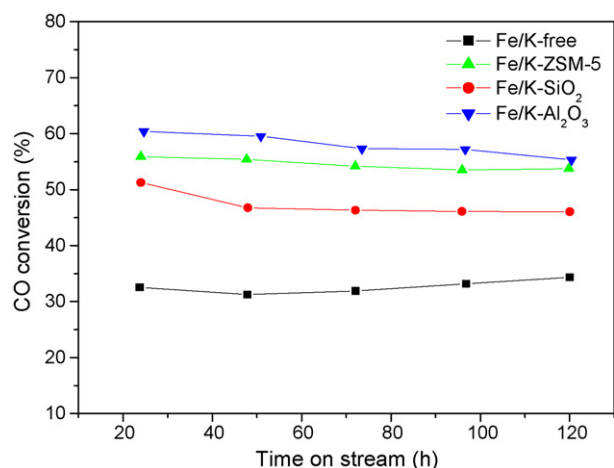**Fig. 4.** Iron phase composition of the catalysts after reaction.

Fig. 5. The carbon monoxide conversion with time on stream for all catalysts.

These results indicate that potassium promoter can facilitate the formation of iron carbide in FTS reaction. And moreover, K–ZSM-5 is less promotional, whereas K–Al$_2$O$_3$ is most effective for the formation of iron carbide.

3.3. Catalytic activity and stability

The carbon monoxide and hydrogen conversions with time on stream for catalysts were shown in Figs. 5 and 6, respectively. It can be seen from Fig. 5 that the addition of potassium promoters can markedly increase the CO conversion. Comparison of the CO conversion results, the Fe/K–Al$_2$O$_3$ catalyst shows the highest FTS activity, next is the Fe/K–ZSM-5, and the K–SiO$_2$ is less promotional on catalytic activity. During the reaction for about 120 h, CO conversion of Fe/K-free catalyst increases slightly with time on stream, whereas those of potassium-promoted catalysts declines to some extent. In detail, CO conversions decline on an even keel from 56% to 54%, 51% to 46%, and 60% to 55% for Fe/K–ZSM-5, Fe/K–SiO$_2$ and Fe/K–Al$_2$O$_3$, respectively. In addition, Fe/K–SiO$_2$ has the lowest CO conversion in all the potassium-promoted catalysts which is possibly due to the presence of acidic sites on silica that offset the electron donating potential of potassium [16]. For the H$_2$ conversion in Fig. 6, the unpromoted catalyst has the lowest conversion and potassium promotion leads to different high H$_2$ conversions with different potassium states. For the stability of H$_2$ conversion,
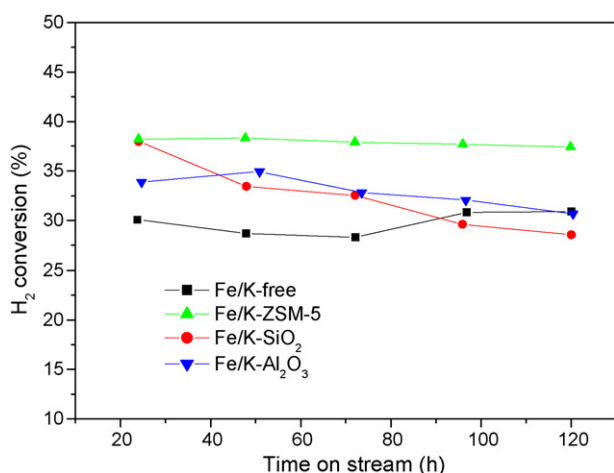
Table 3
Reaction performance of all catalysts for 120 h on stream[a]

Catalysts	Fe/K-free	Fe/K–ZSM-5	Fe/K–SiO$_2$	Fe/K–Al$_2$O$_3$
Time on stream (h)	120.10	119.87	120.08	120.42
CO conversion (%)	34.34	53.73	46.05	55.32
H$_2$ conversion (%)	30.89	37.42	28.56	30.69
CO + H$_2$ conversion (%)	31.94	42.28	33.96	38.12
H$_2$/CO usage ratio	2.05	1.64	1.39	1.28
Q_{WGS}[b]	1.30	2.11	2.58	4.62
Hydrocarbon selectivity[c] (wt%)				
CH$_4$	11.09	9.13	3.82	6.37
C$_2$–C$_4$	25.25	22.89	14.70	18.15
C$_5$$^+$	63.66	67.97	81.48	75.48
Liquid HC	35.67	37.92	17.02	22.98
Solid HC	23.57	23.51	60.15	47.24
C$_{2-4}$$^=$/C$_{2-4}$$^\circ$ (mol)	0.58	0.67	0.77	1.02

[a] Reaction condition: 250 °C, 1.50 MPa, H$_2$/CO = 2.0 and GHSV = 4000 h^{-1}.

[b] $Q_{WGS} = \dfrac{P_{CO_2} \times P_{H_2}}{P_{CO} \times P_{H_2O}}$

[c] Hydrocarbon selectivity are reported on the basis of total hydrocarbon.

Fe/K–ZSM-5 catalyst keeps unchanged basically during the reaction time, whereas those of Fe/K–SiO$_2$ and Fe/K–Al$_2$O$_3$ catalysts reduce gradually from 38% to 28% and 34% to 31%. Potassium combined with different acidic structural promoters all bring higher H$_2$ consumption rate than Fe/K-free catalyst, which is maybe due to the acidic sites of the structural promoters helping the activation and adsorption of H$_2$ in the surface of catalysts, and offering H atoms to FTS catalytic active sites. During the reaction, CO and H$_2$ conversions all lose their activities to some degree, which are 1.0%/day and 1.9%/day for Fe/K–SiO$_2$, 0.4%/day and 0.1%/day for Fe/K–ZSM-5, and 1.0%/day and 0.6%/day for Fe/K–Al$_2$O$_3$, respectively. But for Fe/K-free catalyst, it is an opposite tendency. Besides, it was also found that the loss of activity from the point of view of CO conversion is smaller than that of H$_2$ for Fe/K–SiO$_2$, but the different things happen to the other potassium-promoted catalysts. The results indicate that the different potassium-promoted catalysts may have the different mechanisms in activity loss, and the reason needs a further research.

3.4. Products selectivity

The hydrocarbon selectivities of all catalysts are shown in Table 3 and Fig. 7. It can be seen that the potassium-unpromoted catalyst produces the most gaseous hydrocarbons (C$_1$–C$_4$) and least C$_5$$^+$

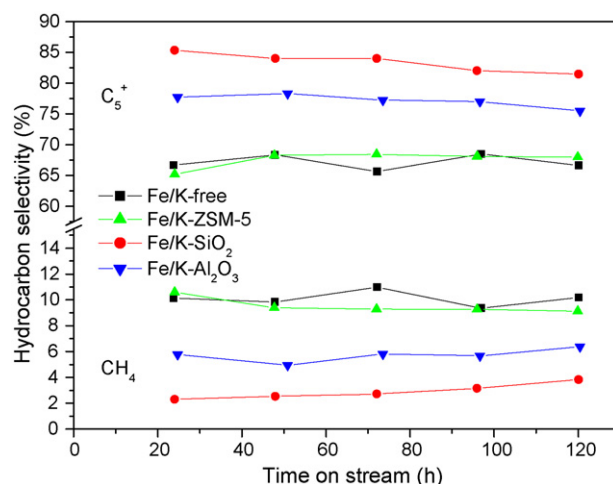**Fig. 6.** The hydrogen conversion with time on stream for all catalysts.

Fig. 7. The hydrocarbon selectivity with time on stream for all catalysts.

products, whereas K promoter restrains the production of C_1–C_4 hydrocarbons and increases the C_5^+ selectivity. Quantitatively, the methane selectivity of Fe/K-free is 11.09% and this value decreases with K promoter in orders: K–ZSM-5 > K–Al_2O_3 > K–SiO_2 (9.13%, 6.37%, 3.82% at 120 h, respectively). Correspondingly, the selectivity of C_5^+ hydrocarbons increase with K promoter in orders: K-free < K–ZSM-5 < K–Al_2O_3 < K–SiO_2 (63.66%, 67.97%, 75.48%, and 81.48%, respectively). The ratios of olefin to paraffin (measured in $C_{2-4}^=$/C_{2-4}°), and liquid and solid hydrocarbon selectivity for all catalysts at 120 h are also listed in Table 3. The values of $C_{2-4}^=$/C_{2-4}° show an apparent increase with promotion of potassium in orders: K–Al_2O_3 > K–SiO_2 > K–ZSM-5. Interestingly, although Fe/K–ZSM-5 catalyst produces comparable light hydrocarbons to Fe/K-free catalyst, it also yields the most liquid hydrocarbons in all catalysts. Fig. 7 also shows the product stability with time on stream. At whole reaction period, Fe/K-free catalyst keeps the methane selectivity at about 10% and C_5^+ hydrocarbons selectivity at about 67%, whereas the hydrocarbon selectivity of K-promoted catalysts varies with time increasing. That is, the methane selectivity of Fe/K–ZSM-5 catalyst decreases and C_5^+ selectivity increases with time increasing. However, for Fe/K–Al_2O_3 and Fe/K–SiO_2 catalysts, the thing is different that methane selectivity increases and C_5^+ decreases with time increasing. The suppressive effect of K promoter on light hydrocarbon and paraffin selectivity is consistent with previous potassium pertinent literature [9,17–21]. Potassium has been reported to enhance CO adsorption but to suppress H_2 adsorption on the iron surface. Hence, changes surface concentrations of C, H species, improves the probability of continued chain growth and the formation of much high molecular-weight hydrocarbons, and inhibits the hydrogenation reaction and the light hydrocarbons and alkanes production.

4. Discussion

It is well known that potassium is used as a chemical promoter in iron-based FTS catalysts. Since potassium is assumed to donate electron to the vacant d orbital of the transition metal as evidenced by the lowering of the metal work function [22], its presence would enhance the dissociation adsorption of CO, while deteriorating the H_2 adsorption [7,22,23]. Therefore, facilitating the reduction of catalysts in CO [7,18,24], and making carburizing process easier at low temperature as seen in Fig. 1. These results are in good agreement with previous studies of potassium-promoted iron catalysts [4,23].

Previous studies [4,23] also revealed that there is a K-support interaction in catalysts, which decreases the promotional effect of potassium on FTS activity and selectivity. The results in this study indicate that the structural promoters absolutely affect the promotional effect of potassium. From the carburization point of view, the potassium combined with Al_2O_3 is more effective while K–ZSM-5 is less. From CO conversion view, K–Al_2O_3 is also more effective while K–SiO_2 is less. From H_2 conversion view, K–ZSM-5 is more effective while K–Al_2O_3 is less at the beginning of reaction and K–SiO_2 at the end of reaction. From hydrocarbon selectivity view, K–SiO_2 is more effective while K–ZSM-5 is less. The different effects of potassium with different structural promoters on carburization, activity and selectivity of catalysts indicate a complex interaction between potassium and structural promoters.

On one hand, basic potassium can interact with the acid sites on structural promoters or is fixed in pores or holes of structural promoters. It is widely proved that SiO_2 does not contain acid sites of either the Brønsted or Lewis type [25–29]. Al_2O_3 contains only Lewis acid sites [29,30] while silica–alumina complex or zeolites (ZSM-5) contain both Lewis and Brønsted acid sites [29–32]. Thereby, these acid sites on structural promoters would decrease

or inhibit the promotional effect of potassium. Although silica does not contain any acid sites, it was added as potassium water glass, potassium interacts strongly with silica. Dry and Oosthuizen [8] also reported that acidic oxides as supports may react with basic alkali and thereby reduce the promotional effect of potassium. McVicker and Vannice [33] reported that a high surface area support tends to reduce the direct contact between iron and potassium, which also renders the potassium promotion less effective. Bukur et al. [9] reported a hydrocarbon selectivity improvement with the addition of support and the results were interpreted in terms of interactions between potassium and/or iron with supports. Jun et al. [13] compared SiO_2 and Al_2O_3 as binders for FTS catalysts and found that the promotion of potassium on the alumina-supported catalyst is much more effective than that on the silica-supported catalyst. That is, a deeper carburization, higher catalytic activity, and lower methane selectivity was observed on alumina-supported catalyst than on silica-supported catalyst. The author thought that alumina has a better dispersion than silica, resulting in a good Fe–K interaction on alumina-supported catalyst and a poor Fe–K interaction on silica-supported catalyst. The results in our study are generally consistent with Jun's results. However, the addition of silica and alumina in this study is via a physical mixture, which is totally different from Jun's preparation method. The physical mixture leads to a poor interaction between iron and structural promoters (silica, alumina, and ZSM-5). In other words, the latter added structural promoters have no contribution on the dispersion of iron and potassium. Therefore, the dispersion effects of structural promoters mentioned by above authors can be withdrawn. Although potassium was added via physically mixing, it apparently varied the catalytic performances of catalysts. The reason is possible due to the migration of potassium on the catalyst surface under FTS reaction conditions. Boes and Böhringer [34] studied the combination of an alkali-promoted iron-based FTS catalyst and an acidic co-catalyst (H–ZSM-5) for syngas conversion to hydrocarbon and found that a physical mixture of the two catalysts resulted in severe alkali migration from the iron catalyst to the zeolite. Similarly, our results indicate that the alkali potassium can easily migrate from the surface or structure of structural promoters (SiO_2, Al_2O_3 and ZSM-5) to the iron surface. At the same time, the different promotional effects of potassium depending on structural promoters indicate that the structural promoters can inhibit the migration of potassium to some extents. From above literature and results, it is clear that ZSM-5 has the strongest inhibiting effect on the motility of potassium while Al_2O_3 is much weaker. Therefore, the amount of effective potassium provided by these potassium-structure-complex promoters is decreased in orders: K–Al_2O_3 > K–SiO_2 > K–ZSM-5, which can well explain the effects of these K-complexes on the carburization of catalysts.

On the other hand, the surface diffusion of reactants and intermediates (called spillover) between the metal sites and the supports or structural promoters can apparently enhance the catalytic activity and vary the selectivity [35,36]. Lots of literature reported a spillover phenomenon of hydrogen, oxygen and carbon monoxide from Pt, Ni, Co, Ru and Rh sites to Al_2O_3 or Zeolite surfaces [37–40] while no such phenomenon was observed on SiO_2 surface [37]. Sen et al. [37,38] studied the CO hydrogenation with physically mixed catalysts of Ni/SiO_2 with Al_2O_3 or Ni/Al_2O_3 with Al_2O_3 and observed a H–CO complex spillover onto Al_2O_3 surface. Especially for the Al_2O_3–Ni/SiO_2 mixture, only one CH_4 site was seen during CO temperature-programmed reaction on Ni/SiO_2 catalysts, but it occurred on Al_2O_3–Ni/SiO_2 mixtures. Zhang et al. [35] studied the hydrogen spillover phenomenon over Pt/H–ZSM-5 catalysts and revealed the occurrence of hydrogen spillover from Pt sites to zeolite acid sites, where hydrogenated the strongly adsorbed pyridine. From above literature and combined with results in this

paper, it is postulated that the spillover phenomenon occurs on the Fe-hybrid catalysts (on the physical mixtures of Fe/K–Al$_2$O$_3$ and Fe/K–ZSM-5, not on Fe/K–SiO$_2$ catalyst). On the Fe/K–Al$_2$O$_3$ and Fe/K–ZSM-5 catalysts, the CO and H species adsorbed on Fe sites transfer to Al$_2$O$_3$ and ZSM-5 surfaces, where the CO species hydrogenates to CH$_4$ and H$_2$O. On the basis of spillover, the enhanced CO and H$_2$ conversions and the increased CH$_4$ selectivity can be well explained. That is, ZSM-5 maybe has the strongest hydrogenation capability for the spilt-over species, which can improve the conversions of CO and H$_2$. At the same time, K–ZSM-5 provides the least effective potassium on catalyst surface. The two factors lead to Fe/K–ZSM-5 producing the highest CH$_4$ selectivity and the highest H$_2$ conversion in three potassium-promoted catalysts. The Fe/K–Al$_2$O$_3$ catalyst contains the most effective potassium and possesses of certain hydrogenation capability, which lead to the highest CO conversion, but medium CH$_4$ selectivity. For Fe/K–SiO$_2$ catalyst, it has a medium effective potassium amount, but no spillover phenomenon and no excessive CH$_4$ formation sites on SiO$_2$ surface. Therefore, Fe/K–SiO$_2$ produces the lowest CH$_4$ products.

5. Conclusion

Iron-based catalysts promoted with potassium combined with different structural promoters have different effects on catalytic performances. The effect of different potassium promoters on carburization of catalysts is in sequence of K–Al$_2$O$_3$ > K–SiO$_2$ > K–ZSM-5 > K-free, according to CO-TPR, XRD and MES. It is because of the different acidic sites on structural promoters and the interaction of potassium and structural promoters. Due to the spillover between the metal sites and the supports or structural promoters, and the least effective potassium on catalyst surface, Fe/K–ZSM-5 catalyst has highest H$_2$ conversion and CH$_4$ selectivity. The Fe/K–Al$_2$O$_3$ catalyst produces the highest CO conversion and medium CH$_4$ selectivity because of the most effective potassium and certain spillover-hydrogenation capability on Al$_2$O$_3$ surface. Fe/K–SiO$_2$ catalyst has a medium effective potassium amount, but no spillover phenomenon and no excessive CH$_4$ formation sites on SiO$_2$ surface, which explain the lowest methane and the highest C$_5^+$ selectivities on the catalyst.

Acknowledgements

References

[1] C.H. Zhang, Y. Yang, B.T. Teng, T.Z. Li, J. Catal. 237 (2006) 405.
[2] W.S. Ning, N. Koizumi, M. Yamada, Catal. Commun. 8 (2007) 275.
[3] A.P. Raje, B.H. Davis, Catal. Today 36 (1997) 335.
[4] Y. Yang, H.W. Xiang, Y.Y. Xu, L. Bai, Y.W. Li, Appl. Catal. A: Gen. 266 (2004) 181.
[5] A.P. Raje, R.J. O'Brien, B.H. Davis, J. Catal. 180 (1998) 36.
[6] S. Li, A. Li, S. Krishnamoorthy, E. Iglesia, Catal. Lett. 77 (2001) 4.
[7] M.S. Luo, R.J. O'Brien, S.Q. Bao, B.H. Davis, Appl. Catal. A: Gen. 239 (2003) 111.
[8] M.E. Dry, G.J. Oosthuizen, J. Catal. 11 (1968) 18.
[9] D.B. Bukur, D. Mukesh, S.A. Pate1, Ind. Eng. Chem. Res. 29 (1990) 194.
[10] H. Dlamini, T. Motjope, G. Joorst, G. ter Stege, M. Mdleleni, Catal. Lett. 78 (2002) 201.
[11] Y. Yong, H.-W. Xiang, L. Tian, H. Wang, C.-H. Zhang, Z.-C. Tao, Y.-Y. Xu, B. Zhong, Y.-W. Li, Appl. Catal. A: Gen. 284 (2005) 105.
[12] A. Kotarba, Catal. Lett. 67 (2000) 129.
[13] K. Jun, H. Roh, K. Kim, J. Ryu, K. Lee, Appl. Catal. A: Gen. 259 (2004) 221.
[14] W.P. Ma, E.L. Kugler, D.B. Dadyburjor, Energy Fuels 21 (2007) 1832.
[15] G.B. Raupp, W.N. Deglass, J. Catal. 58 (1979) 361.
[16] M.E. Dry, T. Shingles, J. Catal. 17 (1970) 341.
[17] R.B. Anderson, The Fischer-Tropsch Synthesis, Academic Press, New York, 1984, p. 145.
[18] H. Schulz, Appl. Catal. A: Gen. 186 (1999) 3.
[19] R.A. Dictor, A.T. Bell, J. Catal. 97 (1986) 121.
[20] H. Arakawa, A.T. Bell, Ind. Eng. Chem. Process. Des. Dev. 22 (1983) 97.
[21] D.G. Miller, M. Moskovits, J. Phys. Chem. 92 (1988) 6084.
[22] N.D. Lang, A.R. Williams, Phys. Rev. Lett. 37 (1976) 212.
[23] H.W. Pennline, M.F. Zarochak, Ind. Eng. Chem. Process. Des. Dev. 26 (1987) 595.
[24] M.E. Dry, T. Shingles, J. Catal. 15 (1969) 190.
[25] E.P. Parry, J. Catal. 2 (1963) 371.
[26] I.D. Gay, S. Liang, J. Catal. 44 (1976) 306.
[27] G. Connell, J.A. Dumesic, J. Catal. 101 (1986) 103.
[28] S. Rajagopal, T.L. Grimm, D.J. Collins, R. Miranda, J. Catal. 137 (1992) 453.
[29] M.I. Zaki, M.A. Hasan, F.A. Al-Sagheer, L. Pasupulety, Colloid Surf. A 190 (2001) 261.
[30] G. Connell, J.A. Dumesic, J. Catal. 102 (1986) 216.
[31] N. Cardona-Martínez, J.A. Dumesic, J. Catal. 125 (1990) 427.
[32] L. Rodríguez-González, F. Hermes, M. Bertmer, E. Rodríguez-Castellón, A. Jiménez-López, U. Simon, Appl. Catal. A: Gen. 328 (2007) 174.
[33] G.B. McVicker, M.A. Vannice, J. Catal. 63 (1980) 25.
[34] F.G. Boes, W. Böhringer, Appl. Catal. A: Gen. 267 (2004) 217.
[35] A. Zhang, I. Nakamura, K. Fujimoto, J. Catal. 168 (1997) 328.
[36] T. Ioannides, X. Verykios, J. Catal. 140 (1993) 353.
[37] B. Sen, J.L. Falconer, T.F. Mao, M. Yu, R.L. Flesner, J. Catal. 126 (1990) 465.
[38] T.S. Zhao, J. Chang, Y. Yoneyama, N. Tsubaki, Ind. Eng. Chem. Res. 44 (2005) 769.
[39] B. Sen, J.L. Falconer, J. Catal. 117 (1989) 404.
[40] B. Sen, J.L. Falconer, J. Catal. 113 (1988) 444.